Hybrid functional study of prototypical multiferroic bismuth ferrite

M. Goffinet, P. Hermet, D. I. Bilc, and Ph. Ghosez
Département de Physique, Université de Liège, B-5, 4000 Sart-Tilman, Belgium
(Received 15 September 2008; revised manuscript received 5 December 2008; published 6 January 2009)

We report a systematic comparison of various exchange-correlation functionals for the prediction of the structural, magnetic, electronic, and dynamical (phonons and Born effective charge tensors) properties of bismuth ferrite, a prototypical multiferroic compound. We have not only considered the usual approximations to density-functional theory such as the local-density approximation (LDA), generalized (GGA), and LDA $+U$, but also hybrid approaches such as B3LYP and B1. The recent B1-WC hybrid functional of Bilc *et al.* [Phys. Rev. B **77**, 165107 (2008)], with the GGA functional of Wu and Cohen and an exact exchange mixing parameter of 0.16, provides very good overall agreement with experiments and can be considered as a valuable alternative to LDA, GGA, and DFT$+U$ for the study of bismuth ferrite. This does not only allow a reliable interpretation of the physical properties of this specific compound but also opens perspectives for further and more predictive first-principles investigations of multiferroic materials.

DOI: 10.1103/PhysRevB.79.014403 PACS number(s): 75.50.−y, 71.15.Mb, 78.20.Bh, 77.80.−e

I. INTRODUCTION

Magnetoelectric multiferroics,[1–3] which combine ferromagnetic (or another kind of magnetic ordering) and ferroelectric orderings, are currently the subject of numerous investigations because they potentially open the way to totally new applications for multistate memories or within the emerging field of spintronics. Especially, bismuth ferrite ($BiFeO_3$) has attracted particular research interest because of its ferroelectric and nearly *G*-type antiferromagnetic orderings at room temperature but also because the study of this prototypical material provides benchmark results, allowing to estimate to which extent different characterization methods can be applied to multiferroics in general. It is in this context that we report an original exchange-correlation (XC) functional-dependent study of $BiFeO_3$.

For usual ABO_3 ferroelectrics, density-functional theory (DFT) has become, already at the local-density approximation (LDA) level, a valuable and predictive investigation tool.[4] *Ab initio* calculations on these materials have not only provided insight into the microscopic origin of ferroelectric phase transitions but can nowadays be effectively applied to complex, even still unsynthesized, nanostructures.[5–7] However, for the study of multiferroics, DFT loses some of its predictive power as one has to go beyond the usual LDA or GGA exchange-correlation functionals. $BiFeO_3$ can already be treated in LDA, but recent studies also make use of LDA$+U$ to improve the description of its electronic properties.[8] It is well known that LDA and GGA strongly underestimate the electronic band gap, which becomes particularly pathological when an insulator is treated as a metal. This is the case for various manganites, as $YMnO_3$ and $BiMnO_3$, which require improved description of the correlation and the use of LDA$+U$ or pseudo-self-interaction correction (pseudo-SIC).[9–12]

As SIC is not commonly available and does not allow, at the time being, self-consistent structural relaxations, LDA $+U$ is often the preferred approach. However, the choice both of the LDA$+U$ formulation and of the related parameters, usually nontransferable, is a semiempirical process associated to a loss of predictive power. Indeed, a common practice is to adjust the parameters in order to reproduce the *experimental* electronic band gap or the *experimental* magnetic moment of a *particular* system, which often leads to different parameter sets. In simple materials, a self-consistently calculated estimate of the U parameter can be given. For instance, for the study of $BiFeO_3$, the value $U_{\text{eff}}=3.8$ eV has been recently determined.[13] However, for more complex and not so well experimentally characterized materials such as double perovskites, it is not known to which extent such parameters can be transferred or how to select parameters for sites occupied by different types of ions. So even if LDA$+U$ has been successfully applied to various multiferroics, an alternative parameter-free approach could be useful for more predictive calculations and also to guide the choice of reliable LDA$+U$ parameters.

Some relatively old studies of magnetic materials point to such an alternative solution that also solves the band-gap problem, namely, hybrid functionals which have so far never been applied to multiferroic materials. As a typical illustration of that, let us consider NiO for which LDA and GGA functionals or pure Hartree-Fock perform quite poorly.[14] Indeed, Hartree-Fock calculations overestimate the electronic band gap and underestimate cohesive energies. LDA yields a 7% too small lattice constant and predicts NiO as a metal despite of the high reported experimental band-gap values of 3.8 and 4.2 eV.[14] The use of GGA opens a gap of only 0.4 eV. Both LDA and GGA, respectively, predict magnetic moments of 1.13 and $1.28\mu_B$, which are significantly lower than the two available experimental values of 1.64 or $1.77\mu_B$.[14] The DFT$+U$ results illustrate a typical dilemma and why it is so difficult to apply this family of functionals to new materials: for $U=6.3$ eV, LDA$+U$ and GGA$+U$ yield correct magnetic moments, but the electronic band gap is of only 3.1 and 3.2 eV, respectively. $U\simeq 8$ eV leads to a correct band gap, but the overall description of the band structure becomes unsatisfactory.[14] The B3LYP hybrid functional, while slightly overestimating the lattice constant, simultaneously predicts correct values of the magnetic moment ($1.68\mu_B$) and electronic band gap (4.2 eV).[14] So, the case of NiO illustrates the failure of traditional XC functionals to correctly describe

magnetic materials and that hybrid functionals such as B3LYP can sometimes be even more accurate than DFT+U functionals.

As B3LYP seems promising for the study of magnetic systems, it is interesting to test its predictive power in multiferroics. However, a recent study has shown that this functional leads to disappointing results in common ferroelectrics such as $BaTiO_3$ and $PbTiO_3$,[15] suggesting that it may not be suitable for the study of multiferroic systems. Fortunately within the same study, a B1-WC hybrid functional, with the generalized gradient functional of Wu-Cohen (WC) and an exact exchange mixing parameter of 0.16, was proposed that gave very good overall results for several physical properties [Born effective charge tensors (Z^*), electronic band gap, cell parameters,…] of various ferroelectric ABO_3 compounds. Our purpose is therefore to test to which extent this very promising B1-WC hybrid functional can also properly describe the properties of $BiFeO_3$ and constitute a valuable alternative to DFT+U methods, allowing a reliable interpretation of physical properties of multiferroics. For comparison, we have also performed LDA+U calculations, using the self-consistently determined value of the Hubbard parameter U.

This paper is organized as follows. In Sec. II, we describe the computational details of our first-principles calculations and give background information on the different functionals used in this paper. Section III presents our computational results. The dependence on the used XC functional of structural parameters, magnetic moment, and electronic structure of $BiFeO_3$ is reported. LDA and GGA calculations are shown and compared to data available in literature before we present our original results obtained with hybrid functionals. Then, we show an XC-functional-dependent phonon calculation together with a comparison of the results to experimental data. We also provide a study of the reliability of each functional to describe the ferroelectric character of $BiFeO_3$ by presenting the zz components of the Z^*. Finally, our results are summarized in Sec. IV. We want to check the transferability of the B1 hybrid functional that has given excellent results in ferroelectric materials and provide at the same time a collection of results for the most important traditional functionals in order to show their respective advantages and drawbacks.

II. COMPUTATIONAL DETAILS

A. First-principles calculations

Most of the presented calculations have been performed using the CRYSTAL06 package.[16] The all-electron Gaussian basis sets used for Fe and O atoms are described, respectively, in Refs. 17 and 18. For Bi atoms, we used the built-in Hay-Wadt large core pseudopotential and the associated basis set given in Ref. 19. The experimental unit cell of $BiFeO_3$ (Ref. 20) was used as an input in the optimization procedure of the structure. The self-consistent cycles are converged up to an energy difference of 10^{-8} Ha (10^{-9} Ha for phonon and Z^* calculations). A $8\times8\times8$ Monkhorst-Pack[21] k-point mesh over the Brillouin zone was found to provide sufficient precision in the calculation of the ground-state geometry, electronic band structure, Z^*, and Hellmann-Feynman forces. All calculations have been performed with spin polarization to reproduce the G-type antiferromagnetic state of $BiFeO_3$.

LDA+U calculations have been performed with Vienna *ab initio* simulation package (VASP) (Refs. 22–24) using the projector augmented-wave (PAW) method. Bi($5d^{10}6s^26p^3$), Fe($3p^63d^64s^2$), and O($2s^22p^4$) electrons have been treated as valence electrons. A $8\times8\times8$ Monkhorst-Pack grid and a 800 eV plane-wave energy cutoff have been chosen. Self-consistent cycles are converged until the energy difference is lower than 10^{-10} eV. The Hubbard parameter, $U_{\text{eff}}=U-J$, defined in the Dudarev formulation and applied on the Fe d orbitals has been set to 3.8 eV, the self-consistently determined value from Ref. 13.

Phonon frequencies, calculated within the harmonic approximation and the *direct method*,[25] have been obtained as follows. First, a geometry optimization of the unit cell of $BiFeO_3$ was performed at lattice parameters obtained from the B1-WC optimization (see Sec. III). Only internal atomic positions were relaxed until the maximum residual forces on the atoms were less than 5.10^{-6} Ha/bohr. Next, from the optimized structure, each atom of the asymmetric unit of $BiFeO_3$ was displaced with an optimal magnitude of 1.10^{-3} Å along the three Cartesian directions. Positive and negative displacements were used to minimize numerical errors related to anharmonic effects. Under these conditions and for each XC functional, 18 distorted structures had been generated to obtain all the Hellmann-Feynman forces required to build the dynamical matrix at the Γ point taking into account the symmetry of the system. Finally, the diagonalization of the dynamical matrix gave access to the square of frequencies and the polarization vectors for each normal mode of vibration. For comparison, we will also report the results at optimized volume from Ref. 26 and results at experimental volume obtained using the same approach.

The Born effective charge tensor, $Z^*_{\kappa,\alpha\beta}$, of atom κ is related to the polarization variation along the Cartesian α direction induced by a rigid displacement, τ, along β of the κ sublattice under zero macroscopic electric field,

$$Z^*_{\kappa,\alpha\beta} = \Omega \left.\frac{\partial P_\alpha}{\partial \tau_{\kappa\beta}}\right|_{\mathcal{E}=0}, \tag{1}$$

where Ω is the unit-cell volume. Z^* have been obtained from finite difference of polarizations as various sublattice displacements are imposed (1.10^{-3} Å) with the electronic part of the polarization computed using the Berry phase method as formulated by King-Smith and Vanderbilt.[27]

B. Description of the used XC functionals

Now, we briefly describe the different XC functionals used throughout this paper. In order to confirm the reliability of the basis sets and the Bi pseudopotential, we used the LDA approximation with the Perdew-Wang (PW)91 parametrization[28] for the correlation and the Dirac-Slater parametrization[29] for the exchange term. For GGA approximations, we used the well-established Perdew, Burke, and Ernzerhof (PBE) parametrization[30] for the XC term, but also the recent and very promising exchange functional proposed

by WC (Ref. 31) in conjunction with the PBE correlation part. In the following of this paper, these different XC functionals are respectively labeled: PW91 (LDA), PBE (GGA), and WC (GGA).

Common hybrid functionals mix a fraction of exact exchange (E_x) with the DFT exchange functional (other mixtures are also possible). Although the adiabatic connection formula[32–34] provides a theoretical basis for mixing usual DFT and exact exchange, the construction of a hybrid functional involves a certain amount of empiricism in the choice of functionals that are mixed and in the optimization of the weight factors given to the exact exchange and DFT terms. In CRYSTAL06, the hybrid B3LYP (Becke, three-parameter, Lee-Yang-Parr)[35,36] exchange-correlation functional is implemented as follows:

$$E_{\mathrm{xc}}^{\mathrm{B3LYP}} = E_x^{\mathrm{LDA}} + a_0(E_x - E_x^{\mathrm{LDA}}) + a_x E_x^{\mathrm{B88}} + E_c^{\mathrm{VWN}} + a_c(E_c^{\mathrm{LYP}} - E_c^{\mathrm{VWN}}), \quad (2)$$

where E_x^{B88} is the Becke 1988 gradient correction for exchange, E_c^{LYP} is the Lee-Yang-Parr gradient-corrected functional for correlation, $E_{\mathrm{xc}}^{\mathrm{LDA}}$ is the uniform electron-gas exchange-correlation energy, and the three dimensionless parameters, determined by Becke, are a_0=0.20, a_x=0.72, and a_c=0.81. As the LYP functional contains already a local part and a gradient correction, one has to remove the local part to obtain a coherent implementation. This can be done in an approximate way by subtracting E_c^{VWN} to E_c^{LYP}. Note that different hybrid functionals can be constructed in the same way by varying the component functionals (for example, by substituting the PBE gradient-corrected correlation functional for LYP) and by adjusting the values of the three parameters.

In addition, we have also considered the B1 simplification,[37] which sets in Eq. (2): $a_x = 1 - a_0$ and $a_c = 1$, i.e.,

$$E_{\mathrm{xc}}^{\mathrm{hyb}} = E_{\mathrm{xc}}^{\mathrm{GGA}} + a_0(E_x - E_x^{\mathrm{GGA}}). \quad (3)$$

The B1-WC functional proposed in Ref. 15 is parametrized with the WC nonlocal exchange part and the PBE nonlocal correlation part and has an exact exchange mixing parameter a_0=0.16. We want to check the predictive power of B1-WC for multiferroic materials by investigating the properties of prototypical $BiFeO_3$.

III. RESULTS AND DISCUSSION

A. Static properties

1. Structural properties

The ground-state structure of $BiFeO_3$ can be seen as a distorted doubled perovskite structure (see Fig. 1) with $R3c$ symmetry presenting simultaneously ferroelectric and nearly G-type antiferromagnetic orders.[20] Atoms of the asymmetric unit occupy the Wyckoff positions labeled 2a and 6b in the rhombohedral system, and are defined as Bi(0,0,0), Fe(x_{Fe},x_{Fe},x_{Fe}), and O(x_{O},y_{O},z_{O}). The structural and magnetic parameters, as well as an estimate of the electronic band gap obtained for different XC functionals, are compared to experimental reference data in Table I.

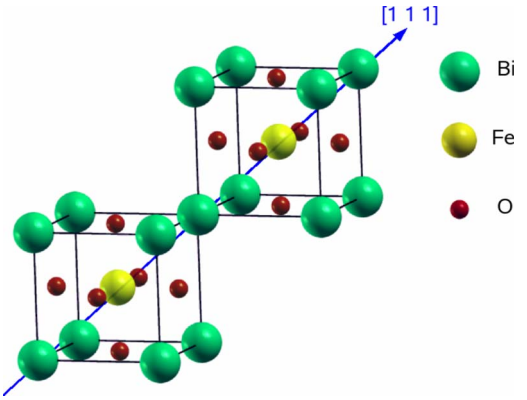

FIG. 1. (Color online) Two undistorted $Pm\bar{3}m$ cubic perovskite unit cells of $BiFeO_3$ sharing a common [1 1 1] diagonal.

First, our structural calculations using PW91 and PBE functionals are in good agreement with those reported in the literature,[8,40] showing *a posteriori* the transferability and the accuracy of the basis sets, and the Bi pseudopotential used in our calculations. PW91 is the only functional predicting a rhombohedral angle greater than the 60° of the ideal perovskite structure and its underestimation of the lattice parameter a_{rh} leads to a unit-cell volume about 5% smaller than the experimental one. The PBE generalized gradient functional yields lattice parameters and a unit-cell volume in better agreement with the experiment and slightly overcorrects the PW91 results. Replacing PBE exchange by WC exchange leads to an even better accuracy in the calculation of the cell parameters, and therefore of the unit-cell volume, compared to local PW91 and semilocal PBE functionals. So, since the computational effort when switching from PW91 to PBE or WC does not increase significantly, the later XC functional should be preferred to perform a structural investigation of multiferroics because it performs equally well as in traditional perovskites. The PW91 functional should however be avoided because it may lead to qualitatively wrong results in the case of strain-dependent investigations. Our LDA+U results are in close agreement with those published in Ref. 8 (U=4 eV), but in less convincing agreement with the experiment than the WC data.

Next, concerning the hybrid functionals, it turns out that the B3LYP functional, which usually predicts very good results in many organic systems,[41] seems less appropriate for the investigation of $BiFeO_3$. Indeed, the rhombohedral angle and lattice parameter are, respectively, underestimated by more than 1° and overestimated by about 0.2 Å, leading to a volume about 7% larger than the experimental one. In addition, x_{O} and y_{O} undergo significant changes with respect to all the other functionals.

Finally, we have investigated the structural properties of $BiFeO_3$ using the B1-WC hybrid functional parametrized with the WC nonlocal exchange part and the PBE nonlocal correlation part. Previous investigations have shown that calculations using an exact exchange mixing parameter of 0.16 are in better agreement with experimentally observable quantities in ferroelectric materials[15] than those based on a theoretically suggested value of 0.25.[42] Our calculations yield the

TABLE I. Dependence of structural parameters, magnetic moment, and electronic band gap with respect to different XC functionals (acronyms defined in Sec. II B). a_{rh}, α_{rh}, and Ω, respectively, denote the lattice parameter, the angle, and the volume of the rhombohedral unit cell. μ_{Fe} is an estimate of the local magnetic moment of the Fe atoms. All calculations have been performed using CRYSTAL06 except the LDA+U calculation which has been performed using VASP. Experimental structural parameters are from Ref. 20 while the experimental magnetic moment (measured on polycrystalline powder) and band gap are, respectively, taken from Refs. 38 and 39.

	LDA	GGA		LDA+U	Hybrids		
	PW91	PBE	WC	U_{eff}=3.8 eV	B3LYP	B1-WC	Expt.
a_{rh} (Å)	5.499	5.697	5.584	5.528	5.808	5.609	5.630
α_{rh} (deg)	60.18	59.20	59.80	59.75	58.27	59.37	59.35
Ω(Å^3)	118.06	128.38	122.55	118.73	133.01	122.99	124.60
x_{Fe}	0.226	0.218	0.223	0.226	0.210	0.219	0.221
x_O	0.522	0.515	0.521	0.540	0.485	0.511	0.528
y_O	0.935	0.925	0.931	0.941	0.915	0.926	0.933
z_O	0.409	0.397	0.403	0.397	0.408	0.406	0.395
μ_{Fe} (μ_B)	3.6	3.9	3.8	4.1	4.2	4.2	3.75
Gap (eV)	0.5	1.0	0.8	2.0	3.6	3.0	~2.5

same conclusion for $BiFeO_3$ so that we focus on results obtained with a mixing parameter of 0.16 (B1-WC). This functional clearly yields the best lattice parameters of all the considered functionals, even if WC-GGA gives slightly better atomic positions. What is perhaps more interesting is that B1-WC is in better agreement with experimental data for both, cell parameters and atomic positions, and performs even better than the LDA+U functional based on a self-consistently determined value of U. This suggests that B1-WC, already shown to be appropriate for usual ferroelectrics, is similarly predictive for multiferroics, at least as long as the structure is concerned.

2. Magnetism

During our systematic studies, an estimate of the local magnetic moment on the Fe atoms was quite straightforward using Mulliken population analysis or integration within a sphere. To the best of our knowledge, the experimental magnetic moment of $BiFeO_3$ has been reported in the literature only on a polycrystalline powder.[38]

The magnetic moment predicted using local PW91 ($\mu_{Fe}=3.6\mu_B$) and semilocal PBE ($\mu_{Fe}=3.9\mu_B$) functionals is in good agreement with the experimental value ($\mu_{Fe}=3.75\mu_B$), whereas WC ($\mu_{Fe}=3.8\mu_B$) yields even better results. All the considered hybrid functionals provide similar values ($\mu_{Fe}\simeq 4.2\mu_B$). Although they slightly overestimate the experimental magnetic moment, essentially because of the exact exchange contributions, the results are in close agreement with the presently and previously reported LDA+U values ($\mu_{Fe}=3.8\mu_B$ for $U=2$ eV and $\mu_{Fe}=4.0\mu_B$ for $U=4$ eV).[8] B1-WC appears also at this level as a good alternative to LDA+U. From our analysis, the WC-GGA results appear as the best compromise between structural accuracy and correct prediction of the magnetic moment, but these conclusions regarding the performance of the different functional classes should be revisited once experimental data on a $BiFeO_3$ monocrystal will be available.

A reliable functional for the characterization of multiferroics should also correctly predict the magnetic ground state. We have therefore performed energy difference calculations between the ferromagnetic and antiferromagnetic configurations using LDA+U and B1-WC. Both functionals yield lower energies for the antiferromagnetic state than for the ferromagnetic state. The energy difference, ΔE, after full structural optimizations is $\Delta E=0.508$ eV for B1-WC and $\Delta E=0.509$ eV for LDA+U. At fixed geometry, these values become 0.536 and 0.529 eV, respectively. So, as far as the magnetic properties are concerned, B1-WC provides results nearly identical to LDA+U and so probably slightly overestimates magnetic interactions.[13]

3. Electronic band structure

As a next step, we have performed electronic band-structure calculations for all the considered XC-functional classes: LDA, GGA, LDA+U, and hybrids. The corresponding estimates of the electronic band gap are reported in Table I. All the functionals correctly reproduce the insulating character of the ground state of $BiFeO_3$. However, the value of the electronic band gap is strongly dependent on the used XC functional and the results are relatively widespread. LDA and GGA functionals significantly underestimate the experimental electronic band gap whereas the hybrid functionals are in much closer agreement.

To the best of our knowledge, no experimental determination of the electronic band gap (E_g) in $BiFeO_3$ monocrystal has been reported in the literature. However, recent papers on nanowires[39] and thin films[43] report an electronic band gap of about 2.5 eV. When admitting that the electronic band gap of $BiFeO_3$ monocrystals is of the same order of magnitude, it once again appears that LDA (0.5 eV) and GGA (0.8–1.0 eV) lead to a significant underestimation. By contrast,

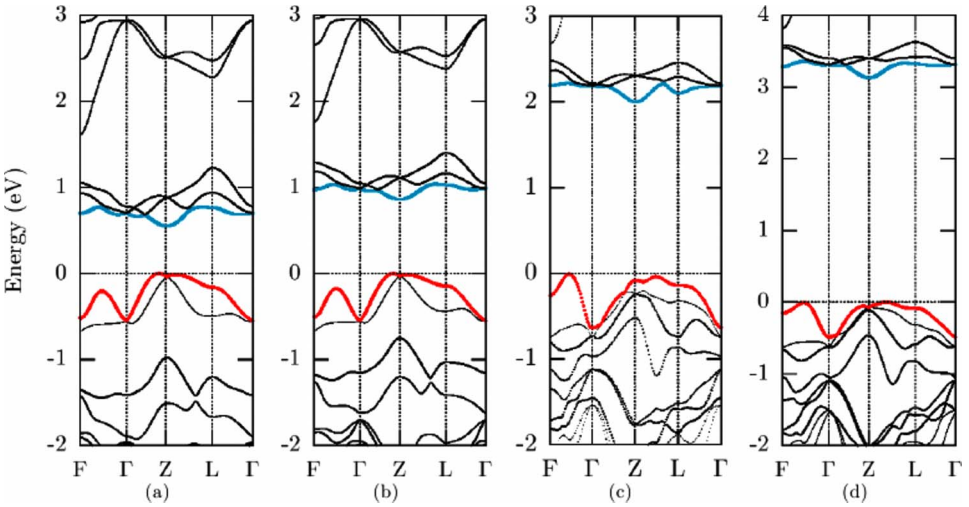

FIG. 2. (Color online) Electronic band structure of $BiFeO_3$ within (a) PW91 (LDA), (b) WC (GGA), (c) LDA+U (PW91, U_{eff} =3.8 eV), and (d) B1-WC (hybrid) functionals. Please note the modified scale in (d). All calculations have been performed using CRYSTAL06 except the LDA+U calculation which has been performed using VASP.

LDA+U and hybrid functionals lead to an electronic band gap in better agreement with the available experimental data, and the prediction obtained using the B1-WC hybrid functional (3.0 eV) seems especially convincing. A very recent theoretical study[44] based on the screened exchange method[45–48] reports E_g=2.8 eV which is comparable to our B1-WC results.

For a given class of functionals (LDA, GGA, or hybrid), the overall shape of the electronic band structure is quite similar, except for a relative energy shift of the conduction and valence bands, leading only to a small difference of the electronic band-gap value. The analysis of the electronic band structure can therefore be restricted to the best XC functionals of each class which are PW91 (LDA), WC (GGA), and B1-WC (hybrid). Figure 2 displays the corresponding electronic band structures along the $F-\Gamma-Z-L-\Gamma$ line. Strikingly, LDA+U and B1-WC band structures are qualitatively very similar and essentially differ by the band-gap value. In particular, we observe that the top of the valence band lies between Γ and Z in PW91 and WC, whereas it is shifted between Z and L for the B1 hybrid functional and LDA+U. Considering the usual accuracy of band-structure calculations, one might however not completely wipe out the possibility that, for the latter functionals, the top of the valence band is located between Γ and F. The bottom of the conduction band is predicted by all the considered XC functionals at Z.

B. Dynamical properties

1. Phonon frequencies

It is well known that some properties such as ferroelectricity and phonon modes are extremely sensitive to the unit-cell volume. Thus, to compute ferroelectricity and phonon modes correctly, the unit-cell volume is often constrained to its experimental value. However, the latter is sometimes not available, especially when predicting new materials or nanostructures. So, it is theoretically more satisfactory to perform calculations without any experimental data adjustment so that the correct prediction of cell parameters previously discussed remains an essential issue. Considering the very good agreement between the B1-WC prediction and the experimental structural parameters of $BiFeO_3$ (see Table I), and to compare rigorously the calculated phonon frequencies with respect to the XC-functional class dependence (LDA, GGA, and hybrids), the lattice parameters (and therefore the unit-cell volume) have been fixed to those obtained using the B1-WC hybrid functional. The corresponding relaxed atomic positions, used for the phonon and Born effective charges calculations, are given in Table II.

Since the rhombohedral phase of $BiFeO_3$ has $R3c$ symmetry, the zone-center phonon modes can be classified into $4A_1 \oplus 5A_2 \oplus 9E$. The A_1 modes are polarized along z, which is aligned along the polar axis of $BiFeO_3$ ([111] pseudocubic direction), whereas the doubly degenerate E modes are polarized in the x-y plane. Both A_1 and E modes are Raman and infrared active while the A_2 modes are silent. To the best of our knowledge, only E-symmetry transverse optical (TO) and A_1-symmetry longitudinal optical (LO) phonon frequencies have been experimentally recorded on a $BiFeO_3$ monocrystal.[50–53] For the best XC functional of each class, TO phonon frequencies of the $R3c$ phase of $BiFeO_3$, obtained using the direct method, are given in Table III [E(TO) modes] and Table IV [A(TO) modes], together with the available experimental data. Previous results obtained at optimized lattice parameters, using the linear-response formalism, PW91 XC functional, and RRKJ optimized pseudopotentials[49] as implemented in the ABINIT plane-wave DFT code,[26] are also reported in Tables III and IV, and differ at most by 15% with respect to those computed at experimental lattice parameters.

Concerning the E(TO) modes, all experimental phonon frequencies are reasonably well predicted by the different XC-functional classes and DFT codes, the lowest deviation between calculation and experiment being clearly for the WC functional, whereas B1-WC slightly overestimates the phonon frequencies which seems to be a typical behavior of hybrid functionals.[41] A relatively good agreement between the different XC functionals and DFT codes is also observed for the A(TO) modes.

Although we have eliminated any volume effects by fixing the lattice parameters (except for the ABINIT calculation

TABLE II. Optimized atomic positions and lattice parameters obtained using PW91 (LDA), WC (GGA), B1-WC (hybrid), and LDA+U (PW91, U_{eff}=3.8 eV) functionals. The two first columns report phonon calculations using PW91 XC functional and optimized pseudopotentials (Ref. 49) as implemented in the ABINIT plane-wave DFT code at optimized and experimental lattice parameters, respectively. These relaxed structures are used for the phonons and Born effective charges computations.

	ABINIT		CRYSTAL06			VASP
	PW91[a]	PW91[b]	PW91	WC	B1-WC	LDA+U
a_{rh} (Å)	5.50	5.63	5.61	5.61	5.61	5.61
α_{rh} (deg)	60.13	59.35	59.37	59.37	59.37	59.37
Ω (Å^3)	117.89	124.60	122.99	122.99	122.99	122.99
x_{Fe}	0.231	0.225	0.221	0.222	0.219	0.221
x_{O}	0.541	0.533	0.514	0.519	0.511	0.531
y_{O}	0.946	0.939	0.931	0.930	0.926	0.926
z_{O}	0.399	0.391	0.406	0.403	0.406	0.401

[a]Optimized volume from Reference 26.
[b]Experimental volume.

at optimized lattice parameters), the different DFT codes give different relaxed structures, which can be at the origin of the observed differences in the phonon frequencies prediction. In Table II, we observe that x_{O}, a parameter that affects the position of all the oxygen atoms, undergoes notable changes when switching from one DFT code (VASP, CRYSTAL06, ABINIT) to another (x_{O}=0.514 using PW91 as implemented in CRYSTAL06 against 0.533 using ABINIT for the same XC functional at very close lattice parameters), leading to different predictions of the frequencies of the modes above 260 cm^{-1} that are mainly dominated by oxygen motions.[26] Furthermore, the frequency of the A_1(TO) mode around 200 cm^{-1} is very sensitive to this effect as its eigendisplacement vectors strongly overlap with an antiferrodistortive rotation of the oxygen octahedra that connects the $R3c$ phase to the ideal perovskite structure.[26]

Thus, the predicted phonon frequencies in the $R3c$ phase of $BiFeO_3$ are very sensitive to the different factors related to the used DFT implementations: basis sets (plane waves or localized orbitals), pseudopotentials (norm conserving or PAW), XC functional (LDA, GGA, hybrids), as well as the used phonon calculation methods (linear response or frozen phonon method). Considering the overall agreement with experimental data for both, the predicted phonon frequencies and the structural parameters, the WC functional appears as the most reliable approach.

TABLE III. Comparison between the phonon frequencies (in cm^{-1}) of the E(TO) modes predicted using PW91 (LDA), WC (GGA), B1-WC (hybrid), and LDA+U (PW91, U_{eff}=3.8 eV) functionals and the experimental ones obtained on Raman (Ra) and infrared (IR) spectroscopies. The two first columns report phonon calculations using PW91 XC functional, RRKJ optimized pseudopotentials (Ref. 49), and linear response as implemented in the ABINIT plane-wave DFT code at optimized and experimental lattice parameters, respectively.

ABINIT		CRYSTAL06			VASP	Expt.			
PW91[a]	PW91[b]	PW91	WC	B1-WC	LDA+U	Ra[c]	Ra[d]	IR[e]	IR[f]
102	89	78	81	79	121	77	75	75	74
152	143	143	145	150	186	136	132	132	134
237	195	226	245	256	251		263	240	240
263	252	246	270	279	271	265	276	264	265
274	267	271	279	289	276	279	295	288	276
335	339	338	346	363	347	351	348	347	346
378	365	359	379	394	380	375	370	369	373
409	381	388	443	480	398	437	441	437	441
509	457	479	526	549	487	525	523	523	522

[a]Optimized volume from Reference 26.
[b]Experimental volume.
[c]Reference 50.
[d]Reference 51.
[e]Reference 52.
[f]Reference 53.

TABLE IV. Phonon frequencies (in cm^{-1}) with their symmetry of A(TO) modes predicted using PW91 (LDA), WC (GGA), B1-WC (hybrid), and LDA+U (PW91, U_{eff}=3.8 eV) functionals. No experimental data are presently available in the literature for the A(TO) modes. The two first columns report phonon calculations using PW91 XC functional, RRKJ optimized pseudopotentials (Ref. 49), and linear response as implemented in the ABINIT plane-wave DFT code at optimized and experimental lattice parameters, respectively.

ABINIT		CRYSTAL06			VASP	
PW91[a]	PW91[b]	PW91	WC	B1-WC	LDA+U	Sym.
109	104	113	115	124	126	A_2
167	163	167	173	171	184	A_1
266	234	202	214	217	246	A_1
261	237	268	276	277	269	A_2
308	288	283	280	309	299	A_2
318	301	313	338	343	316	A_1
446	448	455	452	485	468	A_2
517	491	536	566	603	496	A_1
579	547	579	621	709	609	A_2

[a]Optimized volume from Reference 26.
[b]Experimental volume.

2. *Born effective charges* (Z^*)

Z^* are a fundamental quantity in solid-state physics. They govern the strength of the ferroelectric instability as well as the LO-TO splitting of polar materials. Table V contains, for different functionals, the zz components of Z^* corresponding to a polarization variation along the ferroelectric axis of $BiFeO_3$ induced by an atomic displacement along the same direction. As for the phonon calculations, the cell parameters predicted by B1-WC have been used for all the functionals and the corresponding structures are given in Table II.

First, our PW91 results are in good agreement with previous LDA calculations based on a Berry phase approach.[8] Z^*_{Bi} and Z^*_O in $BiFeO_3$ are particularly functional independent and for Z^*_{Fe} we observe variations lower than $0.3e$. Considering the physical interpretation of Z^* in terms of orbital hybridization changes,[54] a dependence on the band-gap width could have been expected. However, a similar insensitivity of Z^* to the functional has already been highlighted in the functional-dependent study of ferroelectrics.[15] Taking into account recent LDA+U results,[8] we may therefore state that Z^* are quite stable with respect to XC functionals and DFT-based codes. The PBE values of Ravindran *et al.*[40] are much larger than all the results presented in the table and in particular those given by WC. This may be due to an inversion of the $R3c$ and $R\bar{3}c$ structures in their paper. The most important conclusions are that (i) all functionals (LDA, GGA, LDA+U, B1-WC) produce very similar Born effective charges and (ii) the ability of each functional to predict the correct spontaneous polarization is therefore directly related to its ability to reproduce the correct structure (see Sec. III A).

Combining the conclusions of Secs. III B 1 and III B 2, infrared spectra of $BiFeO_3$ obtained from first principles (involving phonons and Born effective charges) are expected to be dependent on the used XC functional, pseudopotentials, and basis sets but mainly because of different phonon predictions, as Z^* are relatively stable.

IV. CONCLUSIONS

In this paper, we have reported the dependence of structural, magnetic, electronic, and dynamical (Z^* and phonons) properties of $BiFeO_3$ with respect to three XC-functional classes (LDA, GGA, and hybrids). First, we have shown

TABLE V. zz components of Z^* provided by CRYSTAL06 using different XC functionals and comparison to reference data reported in literature. The available data reported in literature have been obtained using VASP with the PAW method.

	Present work			Literature		
Atom	PW91	WC	B1-WC	LDA[a]	LDA+U [a]	PBE[b]
Bi	4.27	4.29	4.23	4.28	4.37	4.79
Fe	3.32	3.47	3.66	3.26	3.49	4.86
O	−2.67	−2.67	−2.63	−2.50	−2.61	−3.23

[a]Reference 8.
[b]Reference 40.

that, except B3LYP, all the considered XC functionals provide satisfying structural parameters, the best agreement with experiment being clearly given by WC-GGA and B1-WC hybrid functional. Then, the magnetic moment obtained from a Mulliken population analysis within LDA and GGA is in very good agreement with the experimental value obtained on powder, whereas it is slightly overestimated when using hybrid functionals, which give essentially the same results as LDA+U. Moreover, B1-WC and LDA+U are equally well suited for the prediction of the magnetic ground state and of magnetic coupling constants and thus transition temperatures. In addition, the position of the top of the valence band is dependent on the XC functional and hybrid functionals predict an electronic band gap for $BiFeO_3$ in an at least as good agreement with available experimental data as LDA +U. Phonon calculations present a considerable dependence on the used DFT implementation and framework and on the related structural effects. It nevertheless appears that for phonon calculations, the WC functional should be preferred while B1-WC behaves reasonably well. Finally, our Born effective charge computations have yielded only a very small dependence on the used XC functionals and DFT-based codes, and in particular that B1-WC performs once again quite well.

In addition, it appears from our study that, just as for traditional ferroelectric materials, WC is one of the best functionals to study $BiFeO_3$, its only significant drawback being the description of the electronic structure. This can be solved considering the B1-WC hybrid functional, which correctly predicts structural and dynamical properties and yields, at the same time, a realistic value for the electronic band gap. The B1-WC functional can therefore be considered as a valuable alternative to LDA+U for the predictive study of multiferroics, including not yet well-characterized or hypothetical materials for which the choice of U is sometimes problematic. It could also be considered to provide benchmark results for the adjustment of LDA+U parameters. Finally, B1-WC does not consume huge computational resources and, contrary to pseudo-SIC, allows self-consistent structural relaxations. We are aware that this functional will require additional testing on other multiferroics, but the fact that it performs equally well in several ferroelectrics and in the prototypical multiferroic $BiFeO_3$ is more than encouraging.

ACKNOWLEDGMENTS

M.G. is grateful to FNRS (Belgium). We are grateful to Claude Ederer and Craig Fennie for sharing unpublished results concerning the phonon frequencies of $BiFeO_3$ and for fruitful discussions. Calculations were partly performed at CISM (UCL–Belgium, FRFC Project No. 2.4502.05) and at the Spanish National Supercomputer Center (BSC-CNS). This work was supported by the European STREP project MaCoMuFi and the European Network of Excellence FAME-EMMI.

[1] M. Fiebig, J. Phys. D **38**, R123 (2005).
[2] W. Eerenstein, N. D. Mathur, and J. F. Scott, Nature (London) **442**, 759 (2006).
[3] R. Ramesh and N. A. Spaldin, Nature Mater. **6**, 21 (2007).
[4] K. M. Rabe and Ph. Ghosez, in *Modern Ferroelectrics*, edited by K. M. Rabe, C. H. Ahn, and J.-M. Triscone, Topics in Applied Physics Vol. 105 (Springer-Verlag, Berlin, 2007), pp. 111–166.
[5] C. H. Ahn, K. M. Rabe, and J.-M. Triscone, Science **303**, 488 (2004).
[6] Ph. Ghosez and J. Junquera, in *Handbook of Theoretical and Computational Nanotechnology*, edited by M. Rieth and W. Schommers (ASP, Stevenson Ranch, CA, 2006), Vol. 9, pp. 623–728.
[7] J. Junquera and Ph. Ghosez, J. Comput. Theor. Nanosci. **5**, 2071 (2008).
[8] J. B. Neaton, C. Ederer, U. V. Waghmare, N. A. Spaldin, and K. M. Rabe, Phys. Rev. B **71**, 014113 (2005).
[9] C. J. Fennie and K. M. Rabe, Phys. Rev. B **72**, 100103(R) (2005).
[10] J. E. Medvedeva, V. I. Anisimov, M. A. Korotin, O. N. Mryasov, and A. J. Freeman, J. Phys.: Condens. Matter **12**, 4947 (2000).
[11] B. B. Van Aken, T. T. M. Palstra, A. Filippetti, and N. A. Spaldin, Nature Mater. **3**, 164 (2004).
[12] T. Shishidou, N. Mikamo, Y. Uratani, F. Ishii, and T. Oguchi, J. Phys.: Condens. Matter **16**, S5677 (2004).
[13] I. A. Kornev, S. Lisenkov, R. Haumont, B. Dkhil, and L. Bellaiche, Phys. Rev. Lett. **99**, 227602 (2007).
[14] A. Rohrbach, J. Hafner, and G. Kresse, Phys. Rev. B **69**, 075413 (2004) and references therein.
[15] D. I. Bilc, R. Orlando, R. Shaltaf, G.-M. Rignanese, J. Íñiguez, and Ph. Ghosez, Phys. Rev. B **77**, 165107 (2008).
[16] R. Dovesi, V. R. Saunders, C. Roetti, R. Orlando, C. M. Zicovich-Wilson, F. Pascale, B. Civalleri, K. Doll, N. M. Harrison, I. J. Bush, Ph. DArco, and M. Llunell, *CRYSTAL06 User's Manual* (University of Torino, Torino, 2006).
[17] M. Catti, G. Valerio, and R. Dovesi, Phys. Rev. B **51**, 7441 (1995).
[18] S. Piskunov, E. Heifets, R. I. Eglitis, and G. Borstel, Comput. Mater. Sci. **29**, 165 (2004).
[19] W. R. Wadt and P. J. Hay, J. Chem. Phys. **82**, 284 (1985).
[20] F. Kubel and H. Schmid, Acta Crystallogr. B **46**, 698 (1990).
[21] H. J. Monkhorst and J. D. Pack, Phys. Rev. B **13**, 5188 (1976).
[22] G. Kresse and J. Furthmüller, Phys. Rev. B **54**, 11169 (1996).
[23] G. Kresse and J. Furthmüller, Comput. Mater. Sci. **6**, 15 (1996).
[24] G. Kresse and J. Hafner, Phys. Rev. B **47**, 558 (1993).
[25] K. Parlinski, Z. Q. Li, and Y. Kawazoe, Phys. Rev. Lett. **78**, 4063 (1997).
[26] P. Hermet, M. Goffinet, J. Kreisel, and Ph. Ghosez, Phys. Rev. B **75**, 220102(R) (2007).
[27] R. D. King-Smith and D. Vanderbilt, Phys. Rev. B **47**, 1651 (1993).
[28] J. P. Perdew and Y. Wang, Phys. Rev. B **45**, 13244 (1992).
[29] J. C. Slater, *Quantum Theory of Molecules and Solids 4* (McGraw-Hill, New York, 1994).

[30] J. P. Perdew, K. Burke, and M. Ernzerhof, Phys. Rev. Lett. **77**, 3865 (1996).
[31] Z. Wu and R. E. Cohen, Phys. Rev. B **73**, 235116 (2006).
[32] D. C. Langreth and J. P. Perdew, Solid State Commun. **17**, 1425 (1975).
[33] D. C. Langreth and J. P. Perdew, Phys. Rev. B **15**, 2884 (1977).
[34] O. Gunnarsson and B. I. Lundqvist, Phys. Rev. B **13**, 4274 (1976).
[35] C. Lee, W. Yang, and R. G. Parr, Phys. Rev. B **37**, 785 (1988).
[36] A. D. Becke, Phys. Rev. A **38**, 3098 (1988).
[37] A. D. Becke, J. Chem. Phys. **104**, 1040 (1996).
[38] I. Sosnowska, W. Schfer, W. Kockelmann, K. H. Andersen, and I. O. Troyanchuk, Appl. Phys. A: Mater. Sci. Process. **74**, s1040 (2002).
[39] F. Gao, Y. Yuan, K. F. Wang, X. Y. Chen, J.-M. Liu, and Z. F. Ren, Appl. Phys. Lett. **89**, 102506 (2006).
[40] P. Ravindran, R. Vidya, A. Kjekshus, H. Fjellvag, and O. Eriksson, Phys. Rev. B **74**, 224412 (2006).
[41] W. Koch and M. C. Holthausen, *A Chemist's Guide to Density Functional Theory* (Wiley-VCH, Weinheim, 2002).
[42] J. P. Perdew, M. Ernzerhof, and K. Burke, J. Chem. Phys. **105**, 9982 (1996).
[43] K. Takahashi, N. Kida, and M. Tonouchi, Phys. Rev. Lett. **96**, 117402 (2006).
[44] S. J. Clark and J. Robertson, Appl. Phys. Lett. **90**, 132903 (2007).
[45] D. M. Bylander and L. Kleinman, Phys. Rev. B **41**, 7868 (1990).
[46] K. Xiong, J. Robertson, M. C. Gibson, and S. J. Clark, Appl. Phys. Lett. **87**, 183505 (2005).
[47] J. Robertson, K. Xiong, and S. J. Clark, Phys. Status Solidi B **243**, 2054 (2006).
[48] C. B. Geller, W. Wolf, W. S. Picozzi, A. Continenza, R. Asahi, W. Mannstadt, A. J. Freeman, and E. Wimmer, Appl. Phys. Lett. **79**, 368 (2001).
[49] A. M. Rappe, K. M. Rabe, E. Kaxiras, and J. D. Joannopoulos, Phys. Rev. B **41**, 1227 (1990).
[50] H. Fukumura, H. Harima, K. Kisoda, M. Tamada, Y. Noguchi, and M. Miyayama, J. Magn. Magn. Mater. **310**, e367 (2007).
[51] M. Cazayous, D. Malka, D. Lebeugle, and D. Colson, Appl. Phys. Lett. **91**, 071910 (2007).
[52] S. Kamba, D. Nuzhnyy, M. Savinov, J. Sebek, J. Petzelt, J. Prokleska, R. Haumont, and J. Kreisel, Phys. Rev. B **75**, 024403 (2007).
[53] R. P. S. M. Lobo, R. L. Moreira, D. Lebeugle, and D. Colson, Phys. Rev. B **76**, 172105 (2007).
[54] Ph. Ghosez, J.-P. Michenaud, and X. Gonze, Phys. Rev. B **58**, 6224 (1998).